Applied Sensor Fault Detection and Identification during Steady-state and Transient System Operation

Yu Zhang, Chris Bingham, Michael Gallimore

School of Engineering, University of Lincoln,
Lincoln, LN6 7TS, U.K.
{yzhang; cbingham; mgallimore}@lincoln.ac.uk

***Abstract*— The paper presents two readily implementable methods for sensor fault detection and identification (SFD/I) for complex systems. Specifically, principal component analysis (PCA) and self-organizing map neural network (SOMNN) based algorithms are demonstrated for use on industrial gas turbine (IGT) systems. Two operational regimes are considered viz. steady-state operation and operation during transient conditions. For steady-state operation, PCA based squared prediction error (SPE) is used for SFD, and through the use of contribution plots, SFI. For SFD/I under operational conditions with transients, a proposed 'y-index' is introduced based on PCA with transposed input matrix that provides information on anomalies in the sensor domain (rather than in the time domain as with the traditional PCA approach). Moreover, using a SOMNN approach, during steady-state operation the estimation error (EE) is used for SFD and EE contribution plots for SFI. Additionally, during transient operation, SOMNN classification maps (CMs) are used through comparisons with 'fingerprints' taken during normal operation. Validation of the approaches is demonstrated through experimental trial data taken during the commissioning of IGTs. Although the attributes of the techniques are focused on a particular industrial sector in this case, ultimately their use is expected to be much more widely applicable to other fields and systems.**

***Keywords*— Sensor fault detection and identification; Principal component analysis; Self-organizing map neural network; Steady-state and transient operations.**

I. INTRODUCTION

Complex dynamic systems can typically use many hundreds of sensors for measurement monitoring and control, and themselves account for a substantial proportion of fault modes, whether due to poor connections developing as a result of being subject to long-term vibration or the gradual degradation of their measurement performance due to use in harsh environments. Sensor fault detection and identification (SFD/I) has therefore attracted considerable recent attention by engineers and scientists due to the benefits of reducing down-time and loss of productivity, and increasing the confidence of safety, quality and reliability of systems.

Previously reported SFD techniques include principal component analysis (PCA) and artificial neural networks (ANNs), which have been the most popular candidate solutions. PCA based squared prediction error (SPE) is well established and extensively applied for SFD in industrial processes and power control [1-4]. However, since SPE alone cannot identify which sensor is at fault, additional algorithms have been proposed for SFI; for instance, sensor validity indices (SVI) are introduced in [1,2]. SPE-contribution plots are presented to supplement SPE to diagnosis specific sensor faults in [3,4]. For SFD, ANN techniques are mainly based on multi-layer perceptron neural networks (MLPNNs) or self-organizing map neural networks (SOMNNs). SOMNNs have been successfully reported for fault detection of induction machines [5] and industrial gas turbines [6], with [7] concluding that SOMNNs generally provide good solutions and give better results than approaches based on MLPNNs or other radial basis function neural networks.

Traditional approaches such as PCA based SPE, are suitable when the sensed variables are within a similar range at all times (during steady-state operation), in which case, when a reading falls outside a predetermined 'group average range', it is considered an outlier. However, under operational conditions that are subject to bias and drifting during normal operation (as a result of power or loading changes, for instance), the results from these traditional methods can lead to excessive false alarms being triggered. Here then, a modified PCA-based y-index approach [8], is reported, for groups of sensors that normally exhibit relatively high correlation—shaft bearing vibrations or bearing temperatures in gas turbines, for instance, that is suitable for use under transient operating conditions. Moreover, SOMNN based classification maps (CMs) [9] are also applied for SFD/I on multiple sensor groups with different sensed variables, where SOMNNs arrange high-dimensional data automatically by their topological properties through a 'black-box' approach, and result in numerical classifications.

To provide an application focus to the study, groups of sensors on a 12MW twin shaft industrial turbine unit, are used,

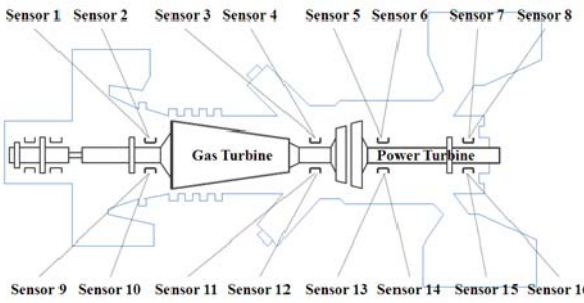

Fig. 1 Bearing vibration and bearing temperature sensor locations on an industrial turbine system

as shown in simplified form in Fig.1. The sensor network in this case include 8 bearing vibration measurements (sensors1—8) and 8 bearing temperature sensors (sensors 9—16) that are sited orthogonally on the inlet and outlet of the gas generator and power turbine shafts.

II. Methodologies

A. Overview of Traditional PCA

PCA is extensively applied for data analysis purposes to reduce a large dataset whilst still preserving 'sufficient' information contained in the original data. Here, the treatment is restricted to a brief overview to introduce terminology and definitions that are subsequently used [10].

Let $\boldsymbol{X}$ be the original data matrix, to describe the original data in principal component space, the following relation is used:

$$\boldsymbol{Y} = \boldsymbol{V}_\alpha^T \boldsymbol{X} , \tag{1}$$

where $\boldsymbol{Y}$ is the principal component matrix, which is a representation of $\boldsymbol{X}$ after PCA, with the ith row representing the ith principal component, and $\boldsymbol{V}_\alpha$ is a basis matrix of $\boldsymbol{V}$. And $\boldsymbol{V}$ represents the eigenvector matrix of the covariance matrix. Since $\boldsymbol{V}_\alpha$ is orthonormal, for a new input data signal, $\boldsymbol{x}$, an approximation of $\boldsymbol{x}$ is then given by:

$$\hat{\boldsymbol{x}} = \boldsymbol{V}_\alpha \boldsymbol{V}_\alpha^T \boldsymbol{x} . \tag{2}$$

PCA generates a principal component sub-space and a residual sub-space. Decomposing the data matrix into two parts, the principal component estimation part, and the residual part, gives

$$\boldsymbol{x} = \hat{\boldsymbol{x}} + \boldsymbol{e} , \tag{3}$$

where the residual can be expressed as

$$\boldsymbol{e} = \left(\boldsymbol{I} - \boldsymbol{V}_\alpha \boldsymbol{V}_\alpha^T\right)\boldsymbol{x} . \tag{4}$$

B. SOMNN

A SOMNN is a competitive learning network [11]. An input data vector, $\boldsymbol{x} = [x_1, x_2, ..., x_I] \in \Re^{I\times 1}$, with I variables (sensors), is associated with a reference vector, $\boldsymbol{r}_i \in \Re^{I\times 1}$, which is often randomly initiated to give each neuron a displacement vector in the input space. For each sample of $\boldsymbol{x}(t)$, $\boldsymbol{r}_w(t)$ constitutes 'the winner', by seeking the minimum distance between the input vector and the reference vector, and is calculated from:

$$\left\|\boldsymbol{x}(t) - \boldsymbol{r}_w(t)\right\| \le \left\|\boldsymbol{x}(t) - \boldsymbol{r}_i(t)\right\| \text{ for } \forall\, i . \tag{5}$$

After obtaining a 'winner', the reference vectors are updated using:

$$\boldsymbol{r}_i(t+1) = \boldsymbol{r}_i(t) + n_{w,i}(t)\left(\boldsymbol{x}(t) - \boldsymbol{r}_i(t)\right), \tag{6}$$

where $n_{w,i}(t)$ is a neighbourhood function, which is normally chosen as Gaussian. The reference vectors are adjusted to match the training signals, in a regression process over a finite number of steps, in order to achieve the final 'self-organizing maps'.

III. SFD/I during Steady-state Operation

An experimental trial showing an emergency fault on sensor 7, during steady-state operation, is shown in Fig.2, which upon further investigation is found to be caused by precision degradation. During steady-state operation, PCA based SPE and SOMNN based estimation error (EE) methods can both be used for SFD/I to provide corroborating evidence of emerging failure.

A. PCA based SPE for SFD/I during Steady-state Operation

The SPE can be obtained by the square of the predicted residual, $\boldsymbol{e}$ in (4), as follows

$$SPE(\boldsymbol{x}) = \left\|\boldsymbol{e}\right\|^2 = \boldsymbol{x}^T\left(\boldsymbol{I} - \boldsymbol{V}_\alpha \boldsymbol{V}_\alpha^T\right)\boldsymbol{x} . \tag{7}$$

Here the eigenvector matrix $\boldsymbol{V}_\alpha$ is calculated from the data history matrix, in this case, the first 300 minutes, which is set to be 'normal'.

The residuals generated by PCA are variances that cannot be modeled in principal component space. When no faults are deemed to be present, the residuals represent normal dynamics and noise in the system, in the PCA residual sub-space. In the presence of a sensor fault, there is divergence of sensor correlations, and the residual vector deviates from the normal range. In this respect, the detection of potential sensor failures is carried out by comparing the SPE with a threshold δ_1 defined by the data history estimation, and the anomaly occurs when

$$SPE > \delta_1 . \tag{8}$$

By way of example, here the threshold is chosen to be a 99.7% confidence level (3 times standard deviation rule). The resulting SPEs are plotted in Fig.3(a) for the experimental trial. It is shown that abnormal conditions are detected after 600 minutes in this case. The individual contributions to the SPE plot, from each sensor, is calculated and viewed as a percentage in Fig.3(b). A greater percentage presents more error contribution from that particular sensor. The error contribution plot is used in conjunction with the SPE plots to

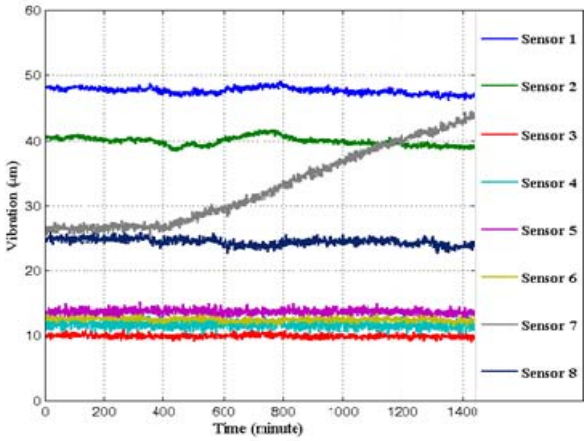

Fig. 2 Experimental trial: vibration information

accomplish SFI after abnormal conditions have been detected. Again, it can be seen that, after 600 minutes, sensor 7 is at fault in this instance.

B. SOMNN based Estimation Error (EE) for SFD/I during Steady-state Operation

SOMNN is performed using the same measurements, with 8 sensor variables and 1440 time samples in the network. To provide the detecting results numerically, an estimation error (EE) is introduced to monitor the performance of the final 'self-organizing maps':

$$EE = \left\| \boldsymbol{x}^{new} - \boldsymbol{r}_w^{new} \right\|, \tag{9}$$

which is defined as the distance between the winning weight vector $\boldsymbol{r}_w^{new}$ and the input vector $\boldsymbol{x}^{new}$ in the new state. If EE is greater than a certain percentage of the normal distribution profile, the new state signal is considered to be abnormal i.e. when

$$EE > \delta_2 . \tag{10}$$

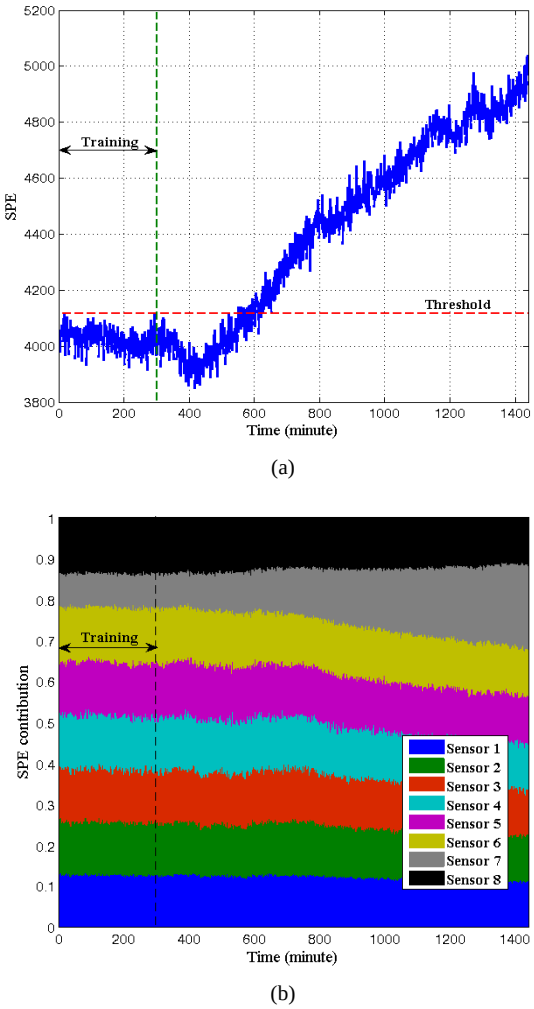

(a)

(b)

Fig. 3 (a) SPE plot. (b) SPE contribution plot for the experimental trial.

In this case the threshold is also selected as a 99.7% confidence level from the training data. The resulting EE plot is shown in Fig.4(a) for the same experimental trial. Here, the fault is detected at 400 minutes.

The EE contribution plot, which represents the percentage of the error each particular sensor contributes to EE, can be used in conjunction with the EE plots to accomplish the SFI after abnormal conditions have been detected, as shown in Fig.4(b). After ~500 minutes, the EE contribution of sensor 7 has significantly increased, which is in agreement with results from PCA based SPE. The sensitivity of EE in this case has produced false alarms on sensor 2.

Both SOMNN based EE and PCA based SPE can perform SFD/I in real-time, but only provide reliable results during steady-state operation, with excessive false alarms occurring when the system is subject to bias or drifting caused by the change of power and load during normal operation, for instance.

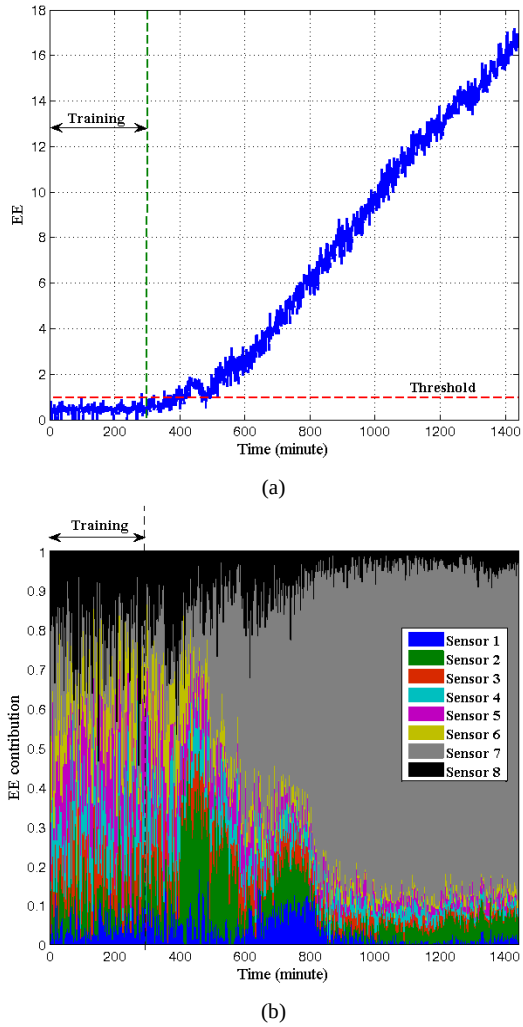

(a)

(b)

Fig. 4 (a) EE plot. (b) EE contribution plot for the experimental trial.

IV. SFD/I during Transient Operational Conditions

A. Introduction of PCA based Y-indices for SFD/I during Operational Transient Conditions

The most important aspects of traditional PCA are the principal components which capture characteristics of the data variance. Denoting $\boldsymbol{X}$ as a matrix of original data, with a dimension of $I \times J$. For traditional PCA methods, the I rows indicate the data from each individual sensor, and J columns incremental time steps from the experiment. In this paper, I is the number of time steps, and J is the number of sensors. To describe the original data in principal component space, the matrix $\boldsymbol{Y}$ in (1) is an $I \times J$ principal component matrix. The first principal component is the first row of the matrix, which contains J values for each sensor. In this case, for a designed time period, the differences between different sensors can be found from the first or the first several $1 \times J$ vectors, assuming it covers sufficient variances of the original data. Let $\boldsymbol{y}_i$ be the ith principal component, and the y-index, $\boldsymbol{d}_{yi}$, is defined as

$$\boldsymbol{d}_{yi} = |\boldsymbol{y}_i| - \min(|\boldsymbol{y}_i|), \tag{11}$$

where $|\bullet|$ refers to the absolute value.

Since the variance is dominated significantly by the first principal component, which allows the threshold for the first y-index to be set to 5 (empirical result) [12], which facilitates graphical sensor fault detection through the first y-index plot in isolation. To use the y-index method, a time-rolling window is employed, as shown in Fig.5. For each time step, a dataset for a total time, t_b, is applied to PCA, and J individually quantifiable numbers describe the differences between the J sensors in the sensor group. The resulting J characteristics are presented to the user on a rolling timeframe, showing changes in sensor behaviour that can be readily identified.

For instance, operation data with transients from 4 bearing vibration sensors, sensors 5—8 in Fig.1, is shown in Fig.6(a). Multiple sensor faults are known to have occurred between 3000 and 6000 minutes. Specifically, a number of high-peak transient noisy readings exist on sensor 5. After further investigation, these high peak noises are caused by transient short-circuiting of the sensor. And prior to 7000 minutes, one high reading on sensor 6 is evident, and several high readings on sensor 8, which are caused by switching of faulted sensor positions by a field engineer during investigations.

When the y-index exceeds the pre-determined threshold, it indicates a sensor fault, and the corresponding faulted sensor is clearly evident as shown in Fig.6(b).

B. SOMNN based CMs for SFD/I during Operational Transient Conditions

Here, SOMNN training is performed initially using the measurements shown in Fig.7, with 16 variables and 1440 time samples (daily data) in the network. To obtain a visual output of the classifications, the SOMNN is first trained with the output space as hexagonal grids, using Matlab Neural Network Toolbox [13]. The weighting matrices in the component planes for the 16 sensors are shown in Fig.8. Each subplot can be considered as a visualization of the weights from the variable (input) to the neurons (output), which can be considered as the deviations of each signal from the 16 sensors' average behaviour. A dark colour on a particular grid indicates a greater correlation between the input and the output, and vice-versa. The component weight planes provide convenient visual interpretations since connection patterns that are similar mean that the variables are highly correlated, and vice-versa. It is evident that there is a clear separation of the weighting matrices between sensors 1 to 8 and sensors 9 to 16 during normal operation. During abnormal operational conditions (depicted in Fig.9), the resulting component planes of the map are shown in Fig.10, where the weighting matrix for sensor 6 is clearly different from that of the other sensors, indicating a sensor fault on sensor 6, which is further investigated to be a loss of electrical connection to this sensor.

To produce the classifications numerically, and hence provide for non-human identification of anomalies from the maps, the SOMNN is trained to classify the data from the 16 sensors into 2 patterns, i.e. instead of 64 neurons in the output layer, here, there are only 2 outputs (with indices 1 or 2). The classification maps for normal operation are shown in CM 1 in Table 1, which shows the separation of the classifications between the bearing vibration sensors (sensors 1 to 8) and the bearing temperature sensors (sensors 9 to 16). Having been trained, the network is applied to data from the unit on a real-time basis to detect deviations from normal behaviour. Specifically, the measurements in Fig.9 are applied to the SOMNN and the 2-classification procedure is applied. The results are shown in CM 2 in Table 1, where sensor 6 is clearly identified as not being classified with the remaining sensors (matching the component planes in Fig.10), and therefore indicates 'abnormal characteristics', as expected in this case.

An advantage of using SOMNNs is that they are simply realized with a basic numeric output. However, the black-box nature of ANNs provides little insight into the relationship between the actual inputs and the ultimate confidence in the final results at the output. Nevertheless, the SOMNN has been shown to be effective as a warning of sensor faults, and for discriminating which sensor is at fault.

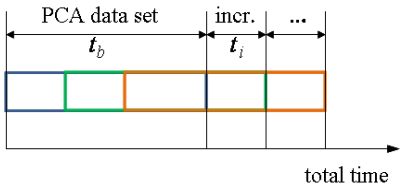

Fig. 5 The concept of PCA time rolling-in system

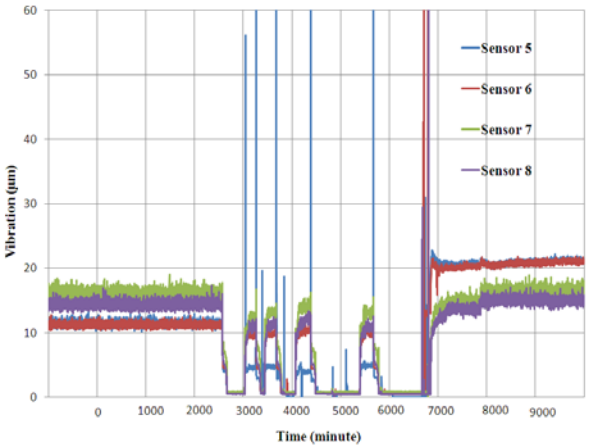

(a)

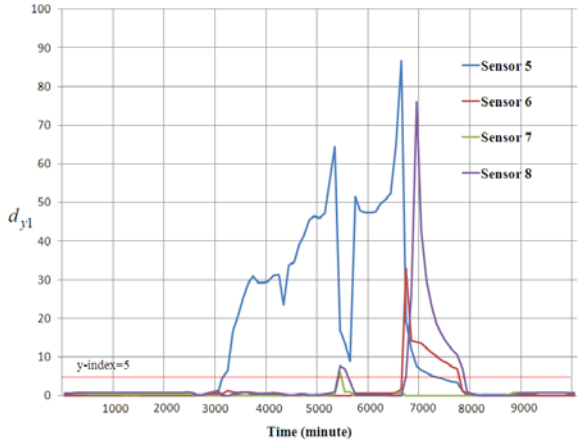

(b)

Fig. 6 (a) Vibration information. (b) Y-index plot indicating sensor faults.

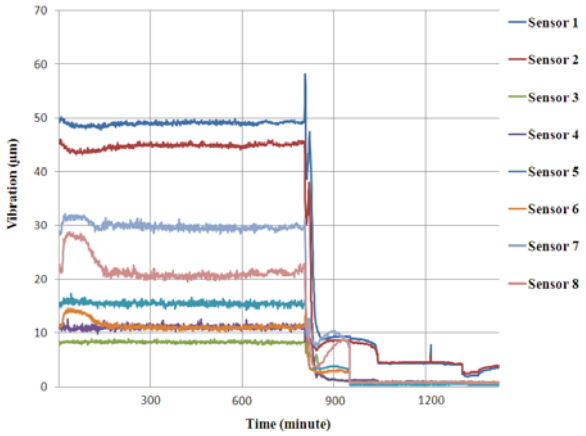

(a)

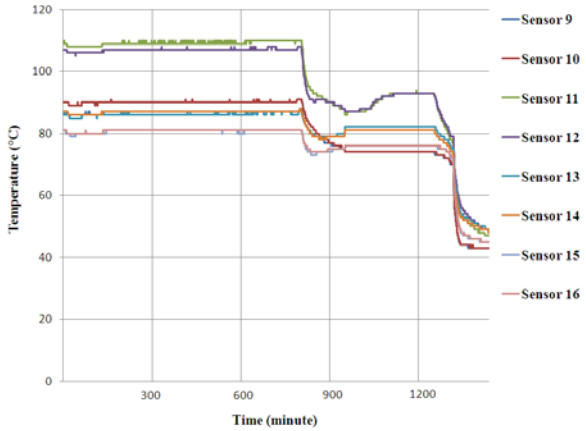

(b)

Fig. 7 Normal operation with transient: (a) Vibration information. (b) Temperature information.

TABLE I
CLASSIFICATION MAPS

Sensor Index	1	2	3	4	5	6	7	8
CM 1	1	1	1	1	1	1	1	1
CM 2	1	1	1	1	1	2	1	1

Sensor Index	9	10	11	12	13	14	15	16
CM 1	2	2	2	2	2	2	2	2
CM 2	1	1	1	1	1	1	1	1

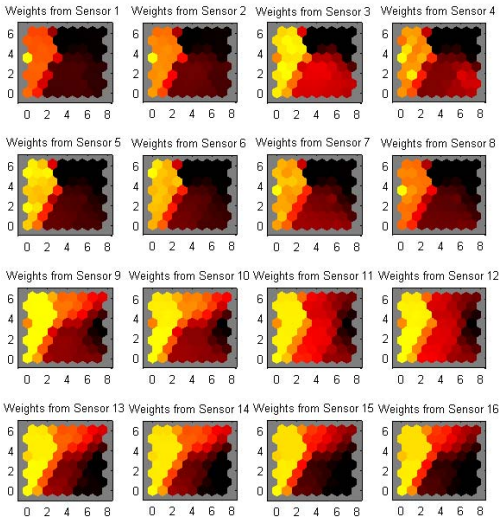

Fig. 8 Component planes of the map for normal operation.

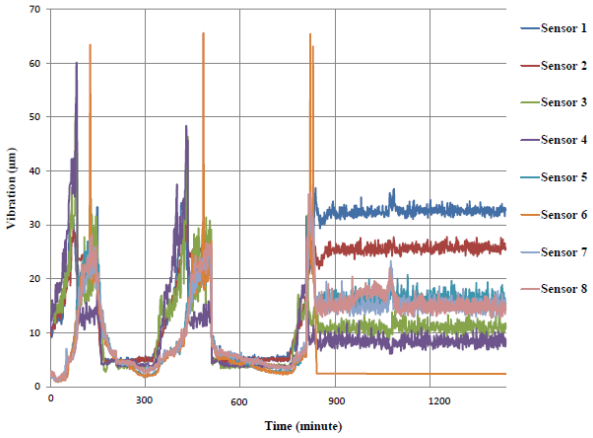

(a)

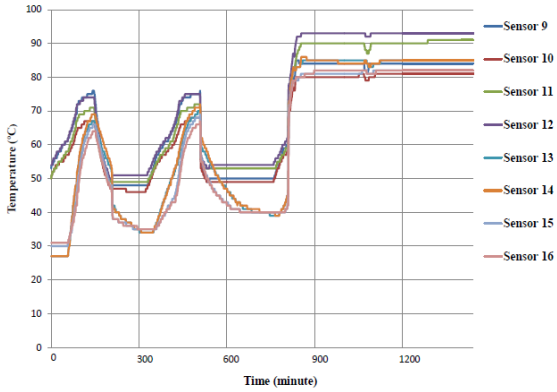

(b)

Fig. 9 Transient operation with sensor fault: (a) Vibration information. (b) Temperature information.

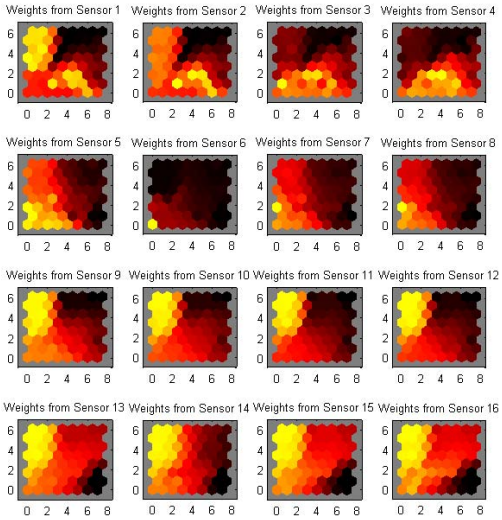

Fig. 10 Component planes of the map showing fault on sensor 6.

V. Conclusions

In this paper, PCA and SOMNN based approaches are applied for SFD/I and faulted sensor data reconstruction, for steady-state operation and operational transient conditions, separately. PCA based SPE and SOMNN based EE and their contribution plots are particularly useful for real-time SFD/I during steady-state operation. For SFD/I during operation with transients, PCA is modified by transposing the input data matrix to seek differences of sensors in a 'sensor domain', while SOMNN is applied by comparing the CMs with known 'fingerprints' of normal operation. Both approaches are shown to be capable of detecting and identify sensor faults successfully through the real time experimental trials on industrial gas turbines, including sensor fault caused by precision degradation, high peak noise sensor fault caused by high voltage short circuits and constant measurement sensor fault caused by loss of connections on sensors. The results are shown to provide comparable results, and can therefore be used together as corroborating evidence of failure.

Acknowledgment

The authors would like to thank Siemens Industrial Turbomachinery, Lincoln, U.K., for providing access to on-line real-time data to support the research outcomes.

References

[1] T. Xu, Q. Wang. "Application of MSPCA to Sensor Fault Diagnosis." *ACTA Automatica Sinica*, vol. 32, No.3, 2006, pp.417-421.

[2] B. Lee, X. Wang. "Fault Detection and Reconstruction for Micro-Satellite Power Subsystem Based on PCA." *Systems and Control in Aeronautics and Astronautics*, vol. 3, 2010, pp.1169-1173.

[3] S. Wang, F. Xiao. "Detection and diagnosis of AHU Sensor Faults Using Principal Component Analysis Method." *Energy Conversion and Management*, vol. 45, 2004, pp.2667-2686.

[4] H. Liu, M. J. Kim, O. Y. Kang, S. B, J. T. Kim, C. K. Yoo. "Sensor Validation for Monitoring Indoor Air Quality in a Subway Station." *Sustainable Healthy Buildings*, vol. 5, 2011, pp.477-489.

[5] L. B. Jack, A. K. Nandi. "Fault Detection Using Support Vector Machine and Artificial Neural Networks Augmented by Genetic Algorithms." *Mechanical Systems and Signal Processing*, vol. 16, No.2-3, 2002, pp. 373-390.

[6] S. Wu, T. W. S. Chow. "Induction Machine Fault Detection Using SOM-based RBF Neural Networks." *IEEE Trans. on Industrial Electronics*, vol. 51, No.1, 2004, pp. 183-194.

[7] K. Elissa, L. F. Gonçalves, J. L.Bosa, T. R. Balen, M. S. Lubaszewski, E. L. Schneider, and R. V. Henriques. "Fault Detection, Diagosis and Prediction in Electrical Valves using Self-organizing Maps." *Journal of Electron Test*, vol. 10, 2011, pp. 1007-1020.

[8] Y. Zhang, C.M. Bingham, M. Gallimore. "Fault Detection and Diagnosis Based on Extensions of PCA," *Advances in Military Technology*, vol. 8, 2013, No. 2, pp.27-41.

[9] Y. Zhang, C.M. Bingham, M. Gallimore. "Applied Sensor Fault Detection, Identification and Data Reconstruction," *Advances in Military Technology*, vol. 8, 2013, No. 2, pp. 13 – 26.

[10] H. Martin, T. Naes, Multivariate Calibration, John Wiley and Sons, New York, 1989.

[11] T. Kohonen, Self-Organizing Maps, Heidelberg: Springer Verlag, 1995.

[12] Y. Zhang, C. M. Bingham, M. Gallimore, Z. Yang, J. Chen. "Applied Sensor Fault Detection and Validation Using Transposed Input Data PCA and ANNs." In *2012 Proc. IEEE Int. Conf. on Multisensor Fusion and Information Integration*, pp. 269-274.

[13] *Matlab version 7.10.0*. Natick Massachusetts, the Mathworks Inc., 2010.